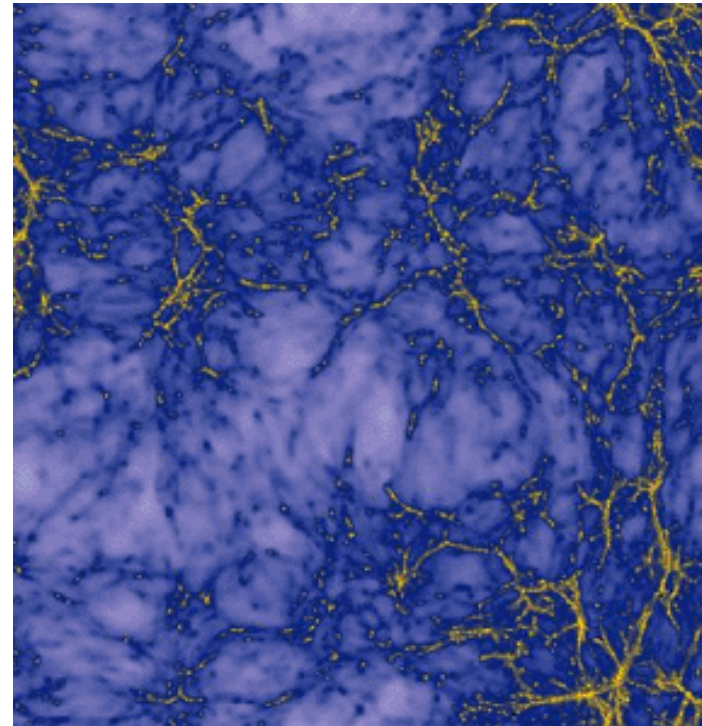
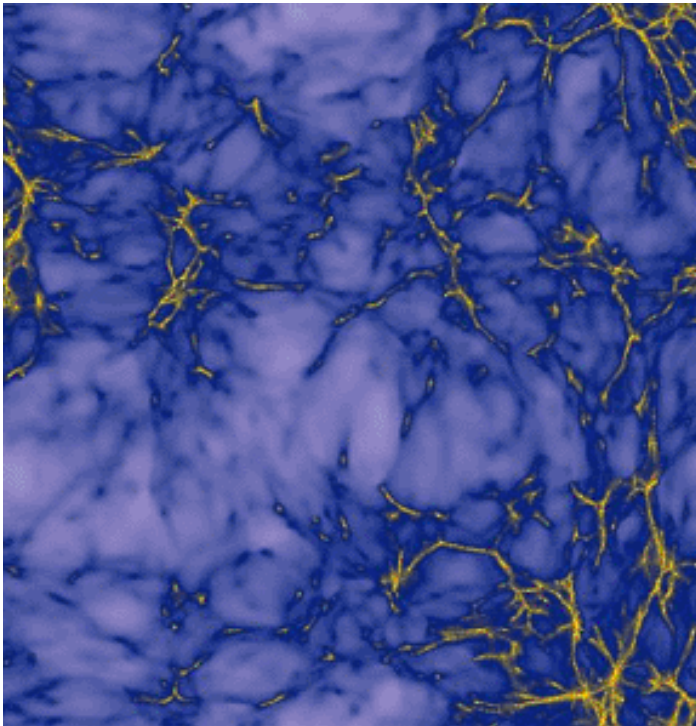


COSMOLOGICAL SIGNIFICANCE of the IGM

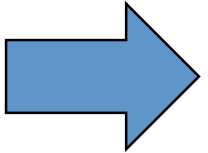
MATTEO VIEL

INAF and
INFN Trieste
(Italy)



OUTLINE: LECTURES

1. Physics of Lyman-alpha and its cosmological relevance
2. Lyman-alpha and fundamental physics
3. IGM/galaxy interplay

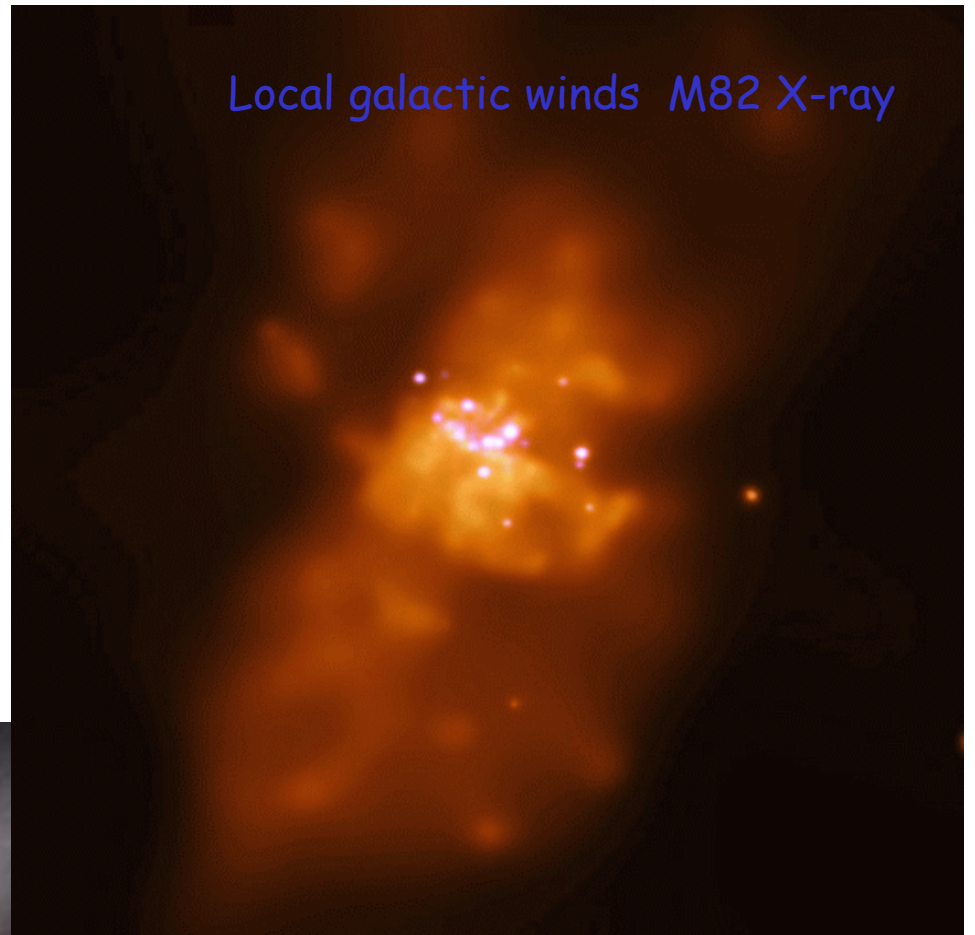


SIMULATING GALACTIC WINDS

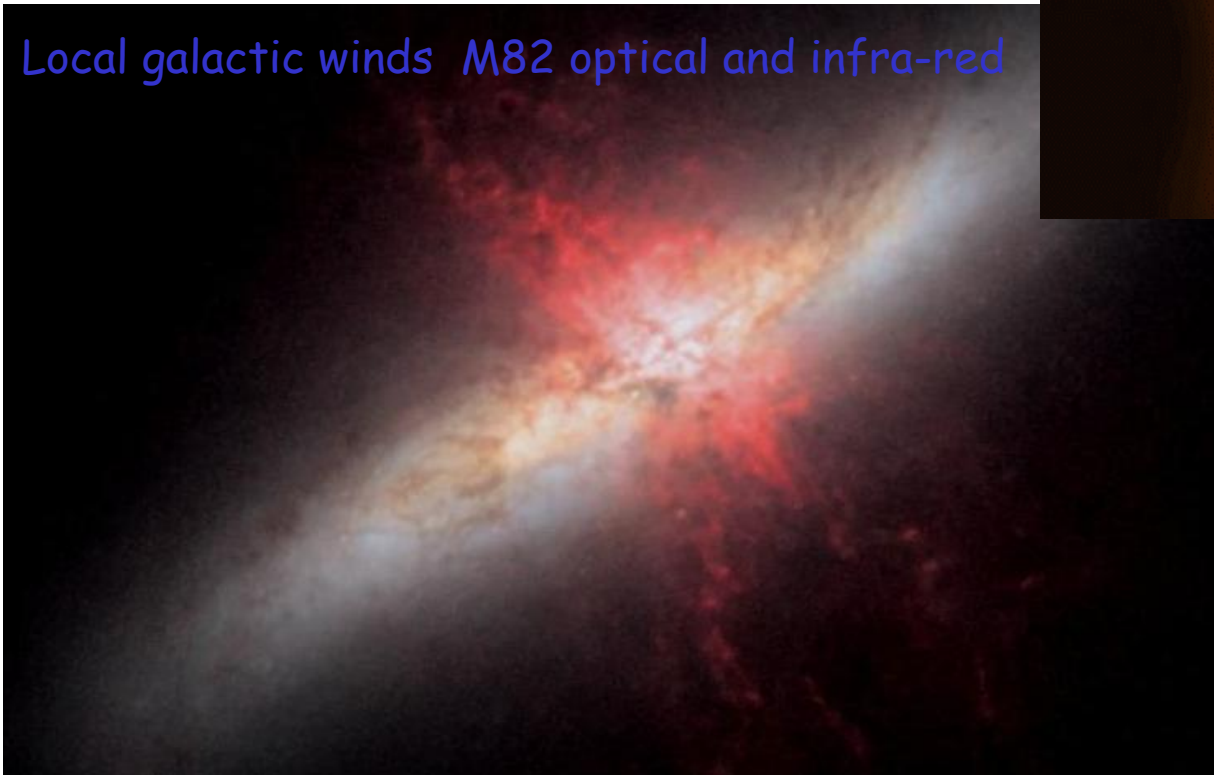
Review on GWs: Veilleux, Cecil, Bland-Hawthorn 2005

Galactic winds -I

Local galactic winds M82 X-ray



Local galactic winds M82 optical and infra-red



Galactic winds -II : Energy driven winds

$$\frac{d\rho_\star}{dt} = \frac{\rho_c}{t_\star} - \beta \frac{\rho_c}{t_\star} = (1 - \beta) \frac{\rho_c}{t_\star}$$

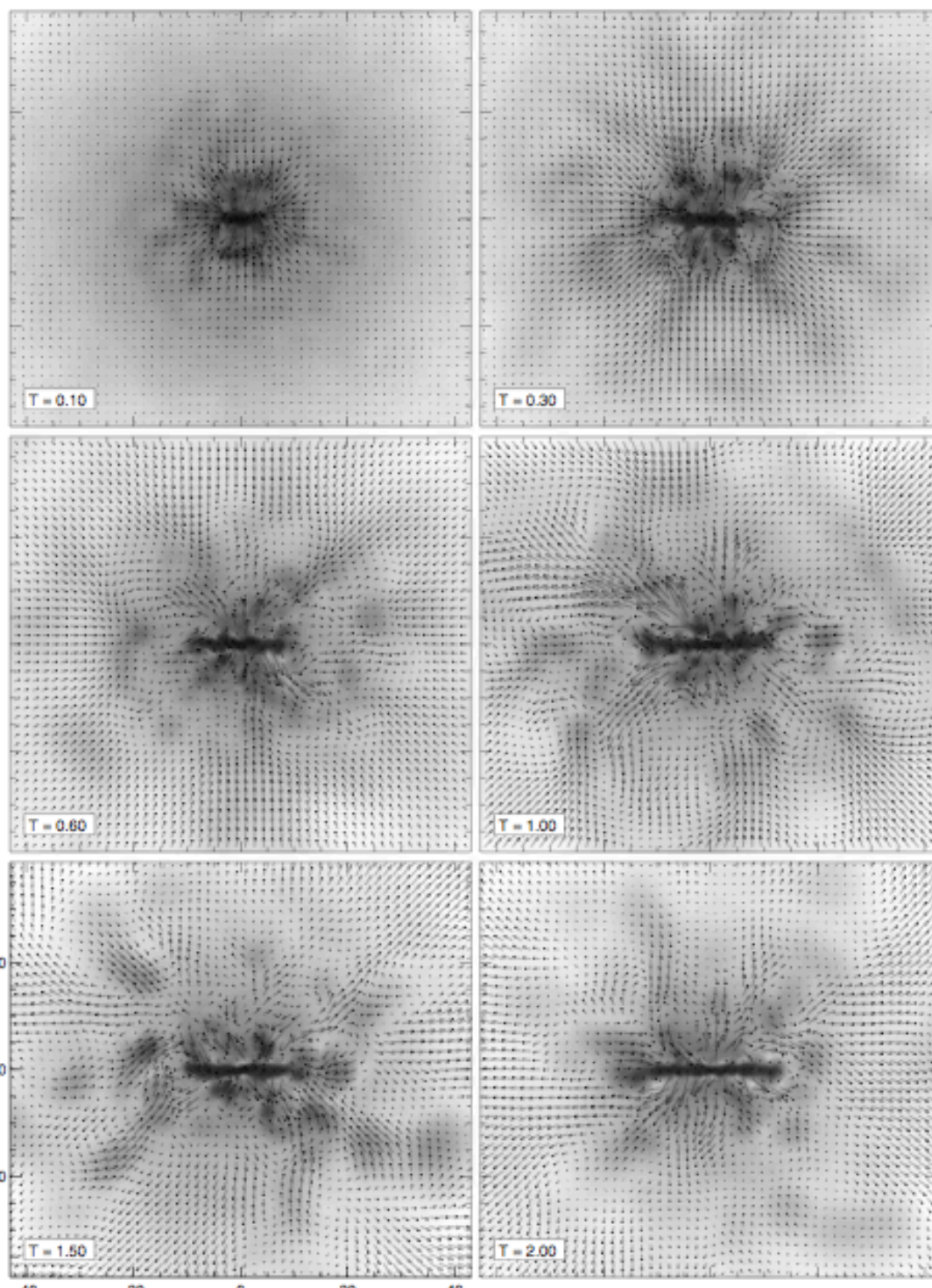
$$\left. \frac{d}{dt}(\rho_h u_h) \right|_{\text{SN}} = \epsilon_{\text{SN}} \frac{d\rho_\star}{dt} = \beta u_{\text{SN}} \frac{\rho_c}{t_\star}$$

$$\dot{M}_w = \eta \dot{M}_\star$$

$$\frac{1}{2} \dot{M}_w v_w^2 = \chi \epsilon_{\text{SN}} \dot{M}_\star$$

$$v_w = \sqrt{\frac{2\beta\chi u_{\text{SN}}}{\eta(1-\beta)}}$$

$$\mathbf{v}' = \mathbf{v} + v_w \mathbf{n}_i$$



Galactic winds -II : Momentum driven winds

$$\dot{M}_W V_\infty \approx \dot{P}$$

$$\dot{P}_{\text{SN}} \sim 2 \times 10^{33} \left(\frac{\dot{M}_*}{1 M_\odot \text{ yr}^{-1}} \right) \text{ g cm s}^{-2}$$

$$L_{\text{SB}} = \epsilon \dot{M}_* c^2$$

$$L_{\text{SB}}/c \sim 2 \times 10^{33} \epsilon_3 \left(\frac{\dot{M}_*}{1 M_\odot \text{ yr}^{-1}} \right) \text{ g cm s}^{-2}$$

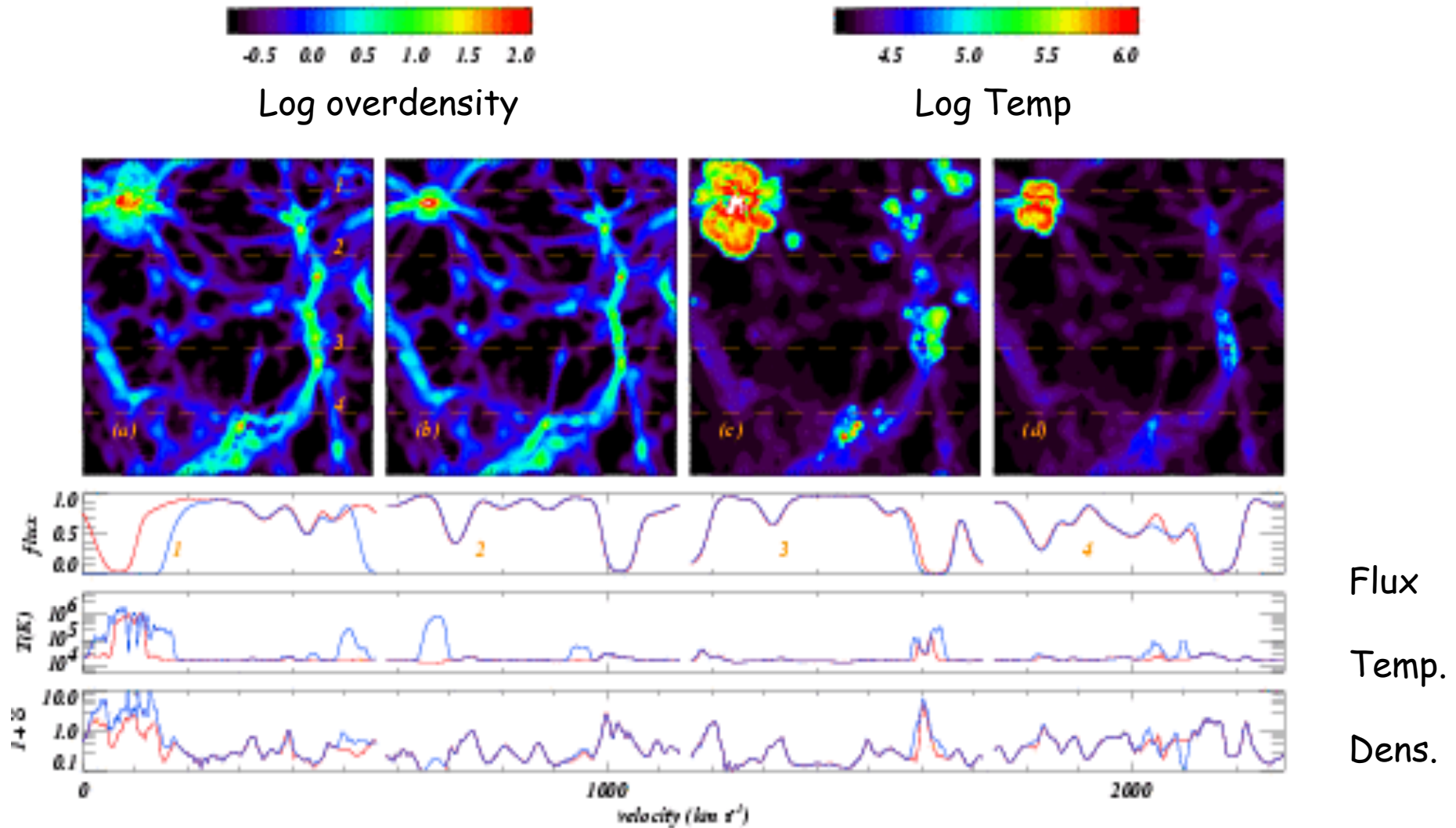
$$\dot{M}_W V_\infty \approx L_{\text{SB}}/c.$$

$$\dot{M}_W \sim \dot{M}_* \left(\frac{\epsilon c}{V_\infty} \right) = \dot{M}_* \left(\frac{300 \epsilon_3 \text{ km s}^{-1}}{V_\infty} \right)$$

Galactic winds: hydro

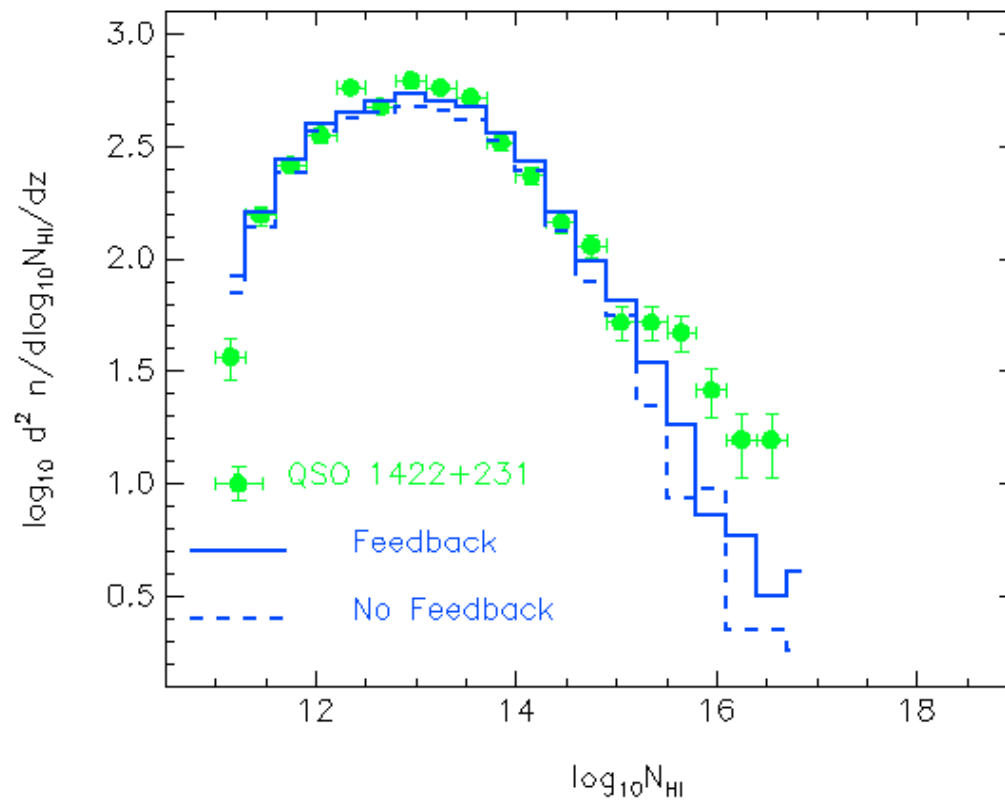
Theory: Galactic winds

do they destroy the forest ?



Theuns, MV, et al, 2002, ApJ, 578, L5

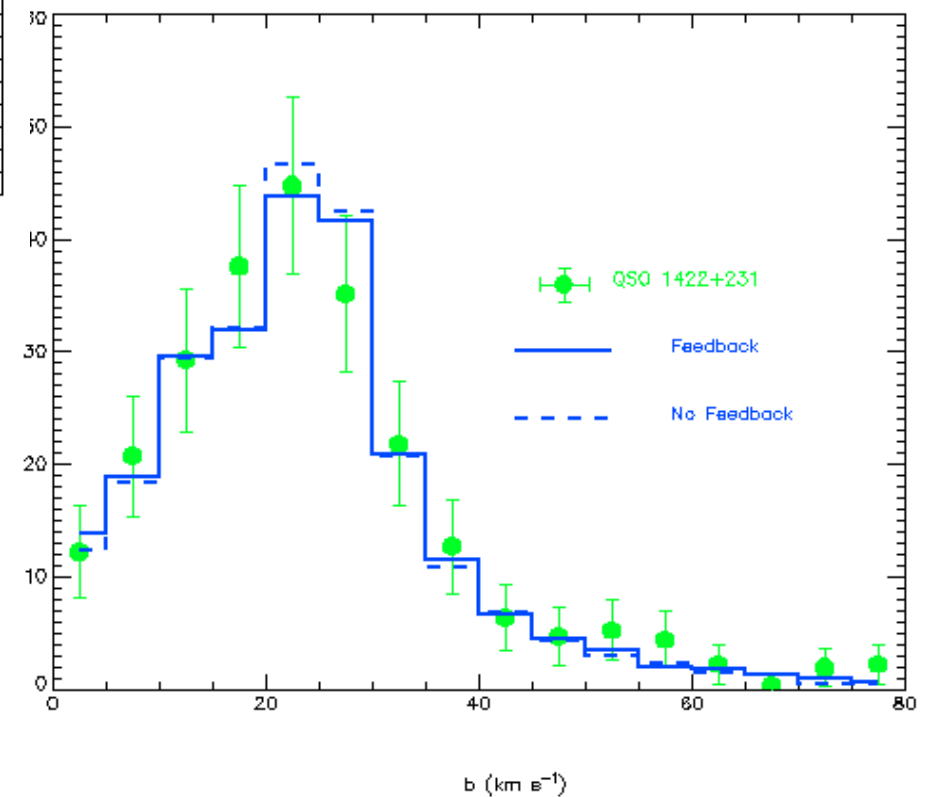
Feedback effects: Galactic winds and HI



Column density distribution function

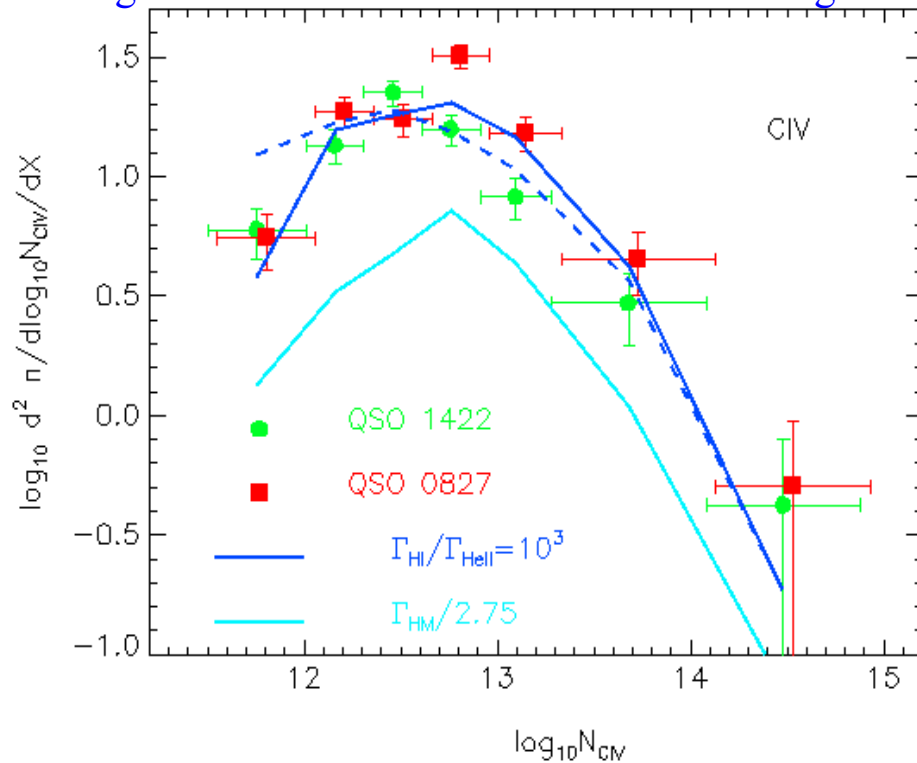
$d^2 n / db$

Line widths distribution



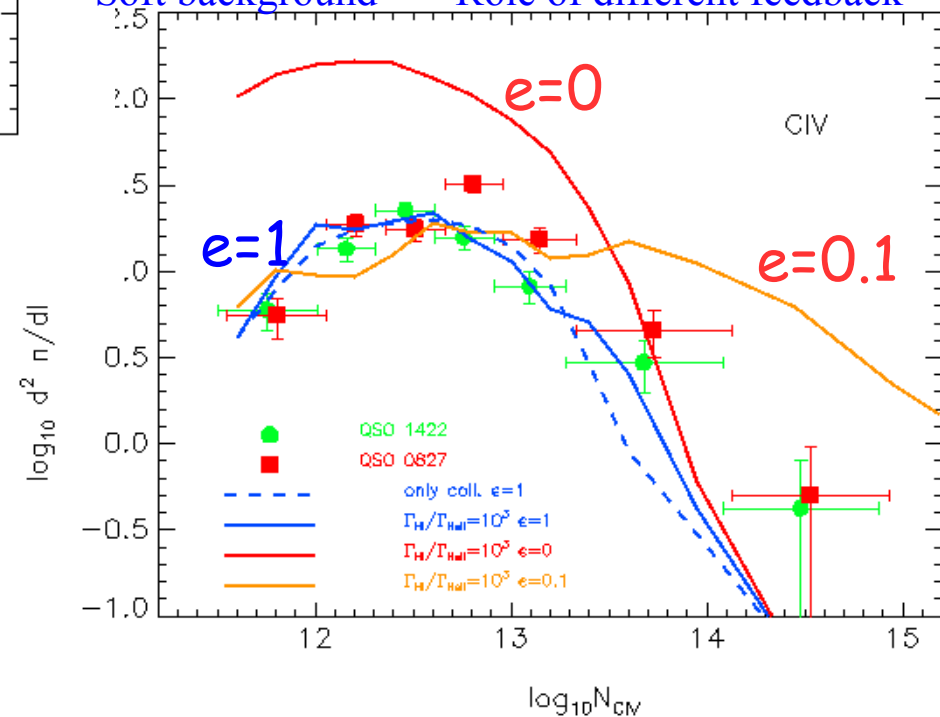
Metal enrichment CIV systems at $z=3$

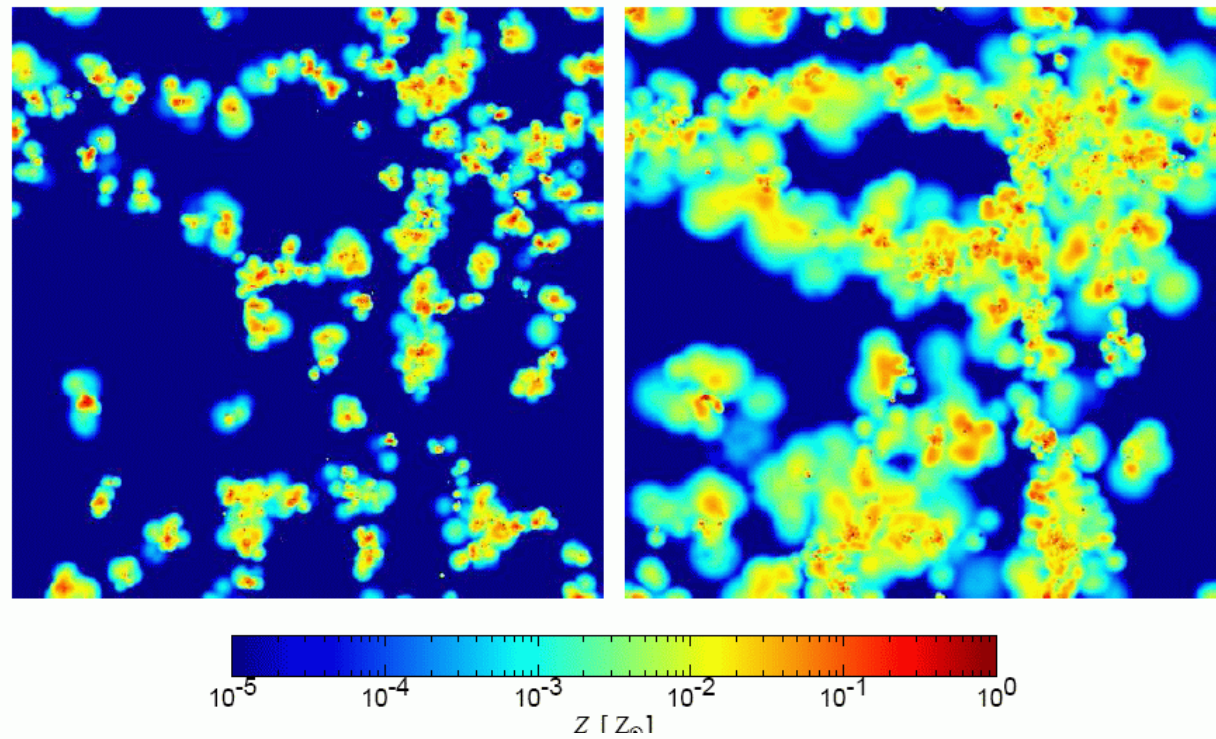
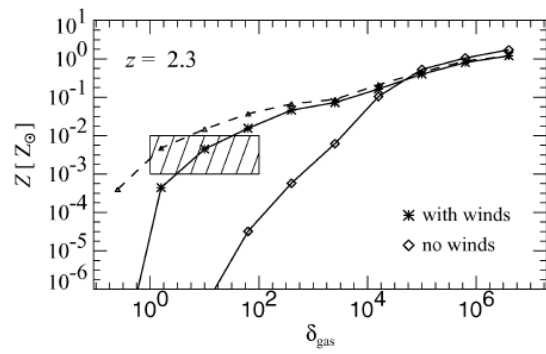
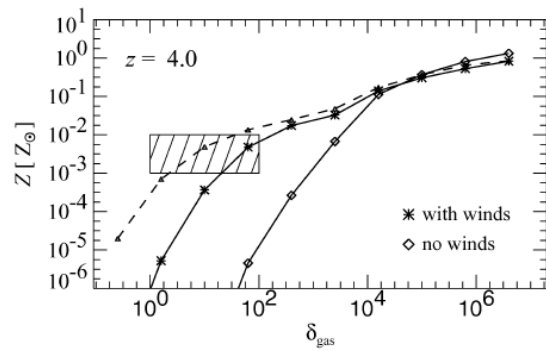
Strong Feedback $\epsilon=1$ ---- Role of the UV background



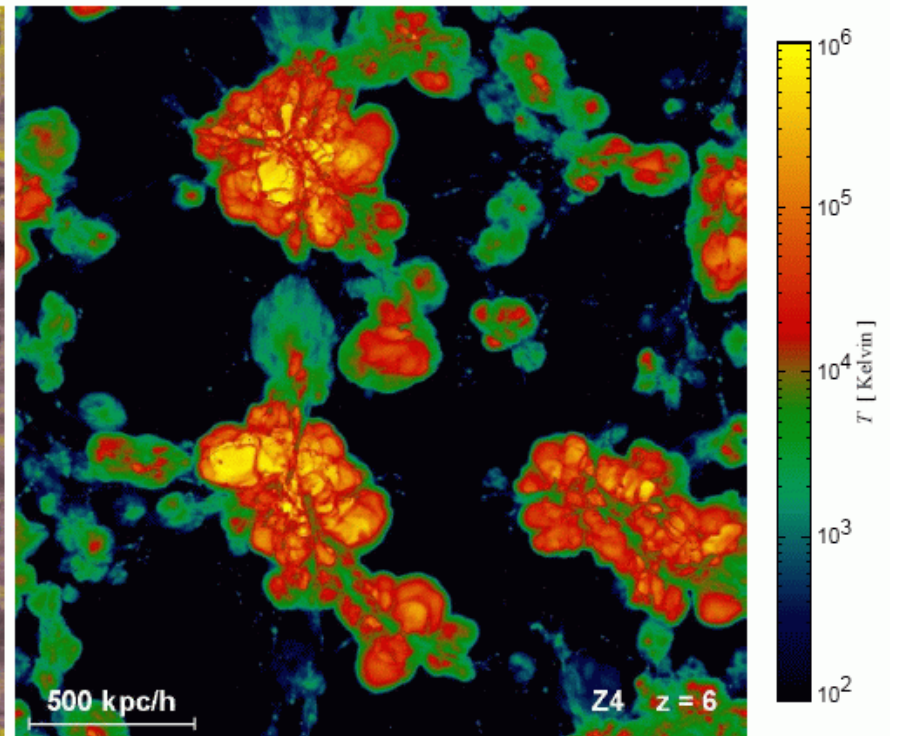
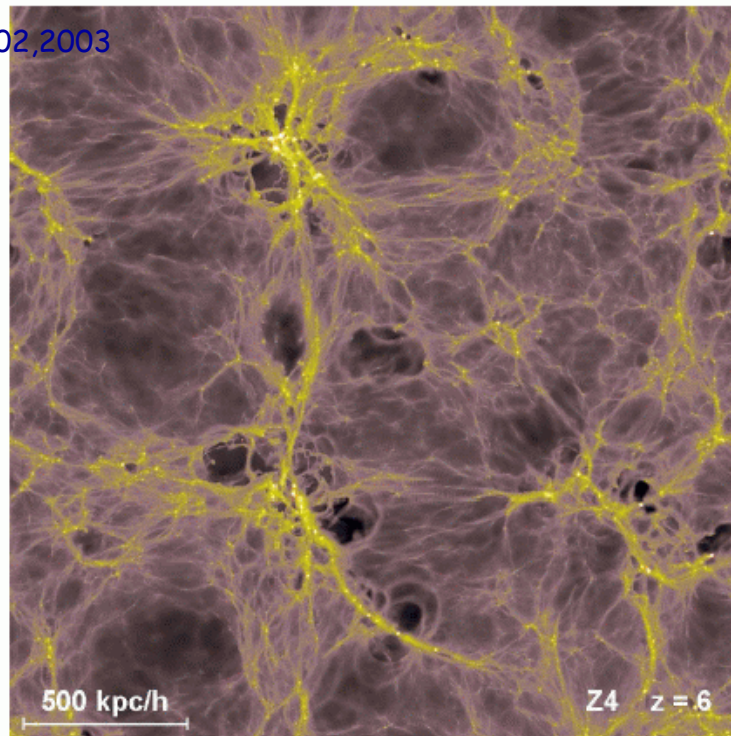
Mori, Ferrara, Madau 2000;
Rauch, Haehnelt, Steinmetz 1996;
Schaye et al. 2003

Soft background ---- Role of different feedback





Springel & Hernquist 2002,2003



Observations: the POD technique

Aguirre, Schaye, Theuns, 2002, ApJ, 576, 1

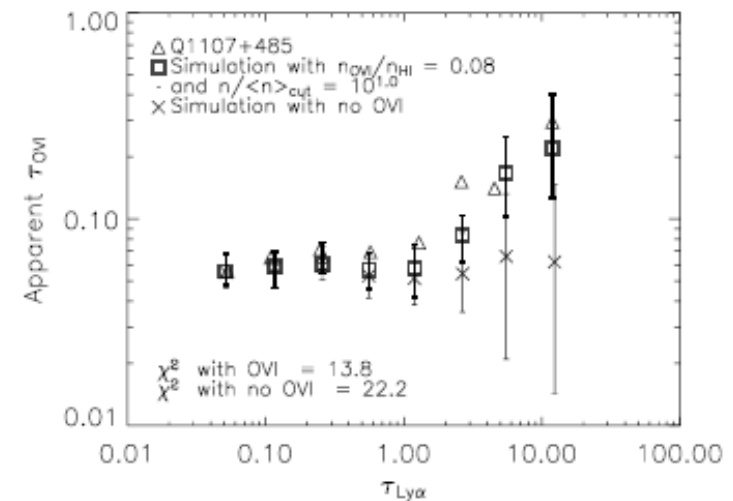
Cowie & Songaila, 1998, Nature, 394, 44

Pieri & Haehnelt, 2004, MNRAS, 347, 985

Pixel-by-pixel search using higher order transitions

$$\tau_{\text{Ly}\alpha}^{\text{rec}} = \min\{\tau_{\text{Ly}\alpha} f_{\text{Ly}\alpha} \lambda_{\text{Ly}\alpha} / f_{\text{Ly}\alpha} \lambda_{\text{Ly}\alpha}\}$$

$$\tau_{\text{OVI}} = \min\left(\tau_{\text{OVIa}}, \frac{f_{\text{OVIa}} \lambda_{\text{OVIa}} \tau_{\text{OVIb}}}{f_{\text{OVIb}} \lambda_{\text{OVIb}}}\right)$$



Observations: the POD technique-II

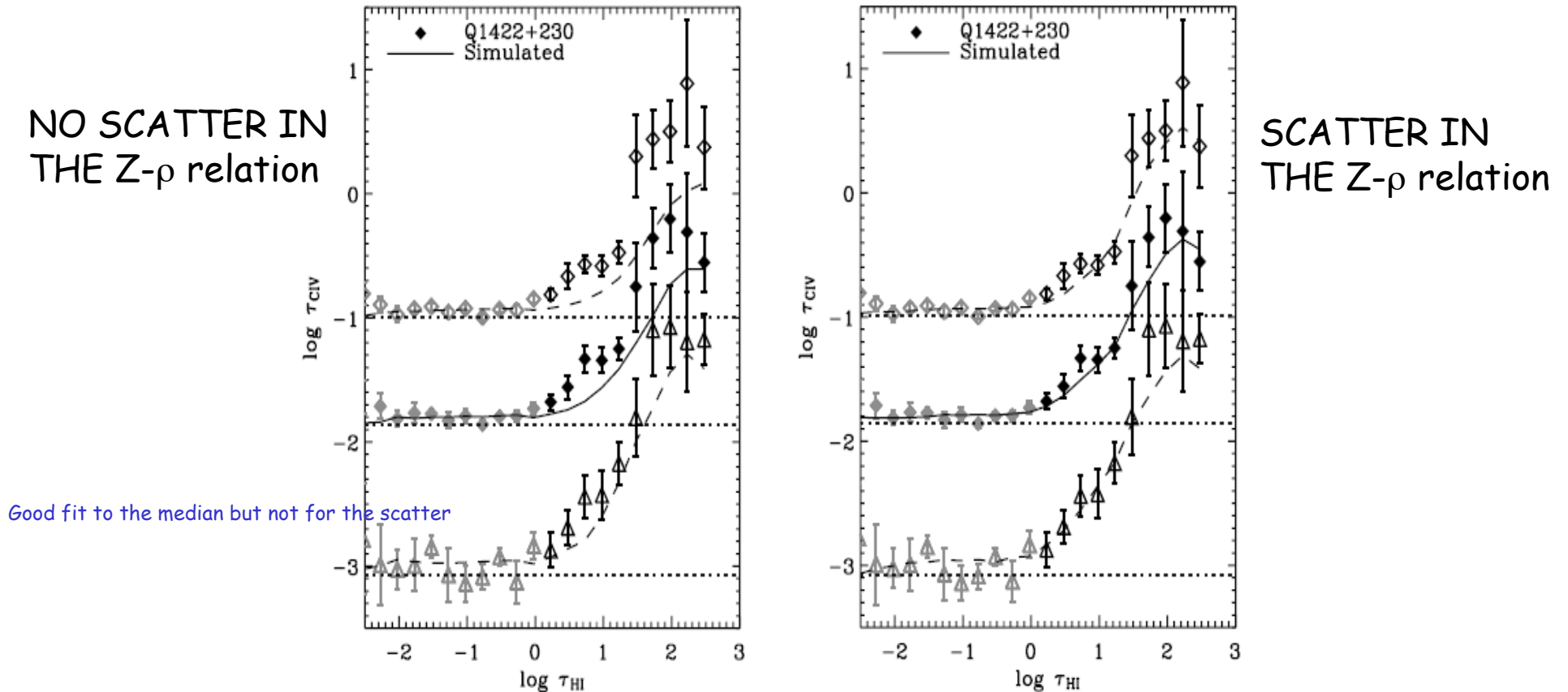
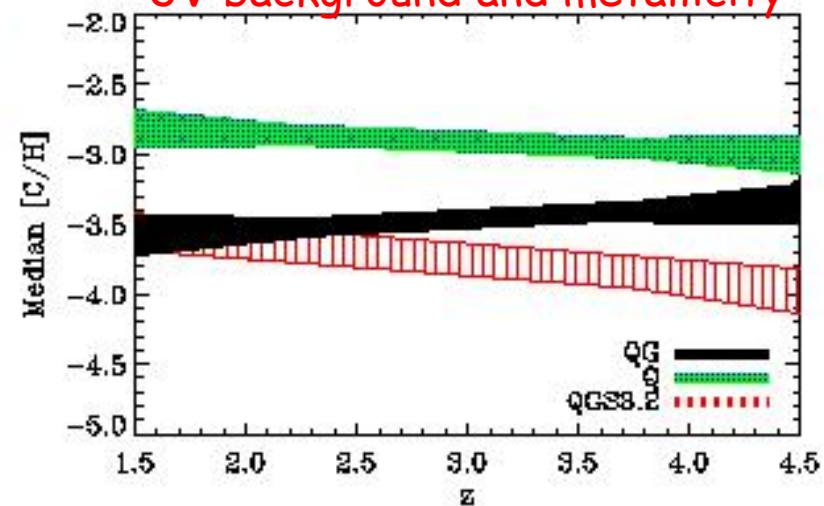
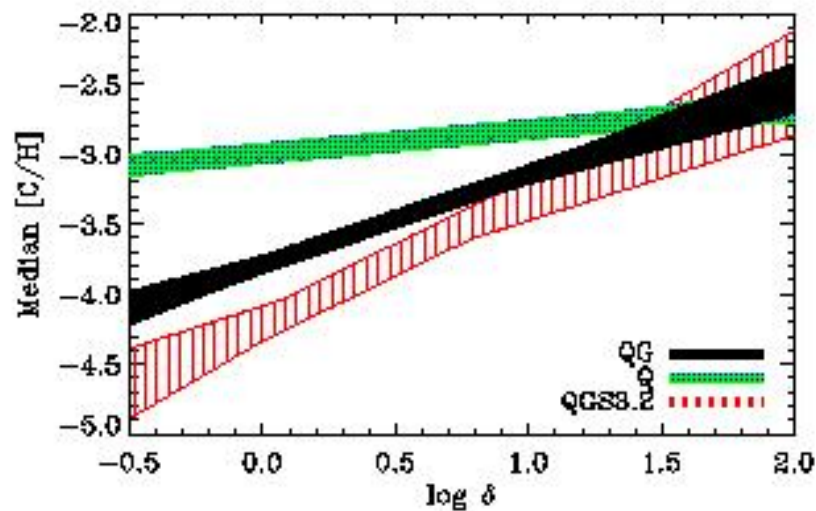


FIG. 5.—Comparison of the optical depth statistics of observed and simulated spectra using the metal distribution measured from the observations. From top to bottom the three sets of data points are the 84th (*open diamonds*), 69th (*solid diamonds*), and 50th (*triangles*) percentiles of the recovered C iv optical depth as a function of $\tau_{\text{H I}}$ for Q1422+230. For clarity, the 84th and 69th percentiles have been offset by +1.0 and +0.5 dex, respectively. The curves in the left-hand panel are for a simulation in which each particle was given the median metallicity measured from the observations, $[C/H] = -3.12 + 0.90(\log \delta - 1.0)$. The simulation can fit the observed median $\tau_{\text{C IV}}$ (χ^2 probability $Q = 0.21$), but not the observed $\tau_{\text{C IV}}(\tau_{\text{H I}})$ for the other percentiles ($Q < 10^{-4}$). The curves in the right-hand panel are for a simulation that has the same median metallicity, but which includes scatter. The simulation cube was divided into 10^3 cubic sections, and all particles in each section were given a metallicity of $[C/H] = -3.12 + s + 0.90(\log \delta - 1.0)$, where s , which is the same for all particles in the subvolume, is drawn at random from a lognormal distribution with mean 0 and variance $\sigma = 0.81$ dex as measured from the observations. The simulation provides an acceptable fit to all percentiles (from top to bottom, $Q = 0.33, 0.69$, and 0.90).

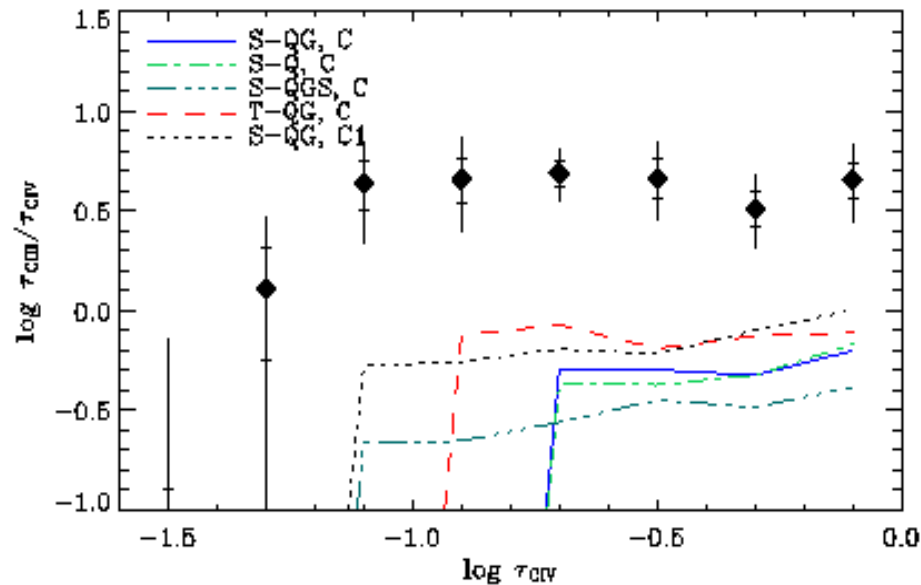
POD technique and proximity -IV

UV background and metallicity



Schaye, Aguirre et al. 2004,2005

Still problems from simulations?



Aguirre et al. 2006

SIMULATIONS' PROBLEM:
ENRICHED GAS IS

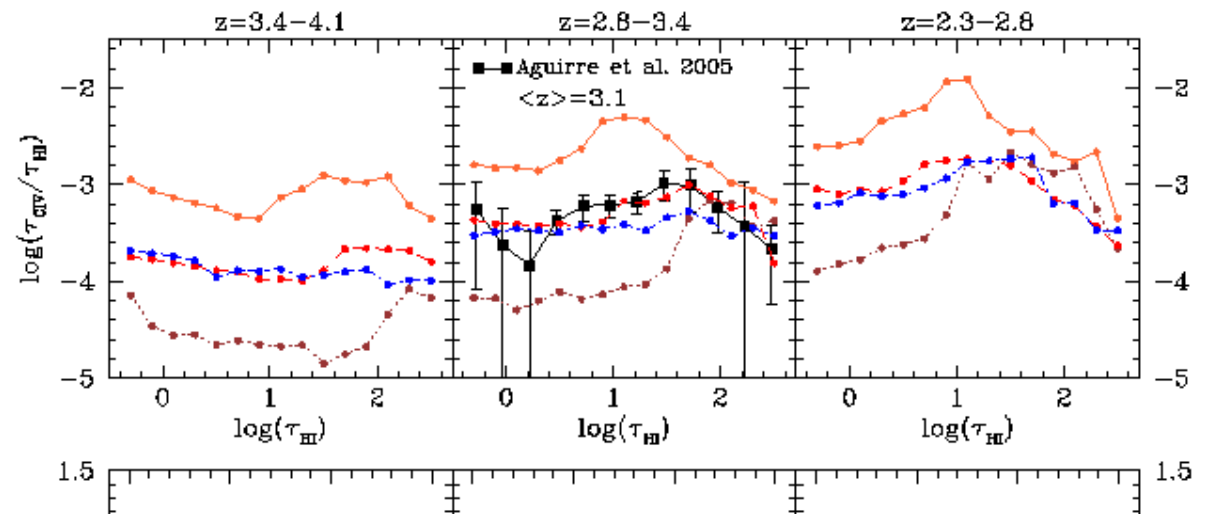
- 1) TOO HOT
- 2) NOT DENSE ENOUGH
- 3) TOO INHOMOGENEOUSLY DISTRIBUTED

Oppenheimer & Dave', 2007
Dave' & Oppenheimer, 2009

Energy driven $\frac{1}{2}\dot{M}_w V_\infty^2 \approx \dot{E}$
Momentum driven $\dot{M}_w V_\infty \approx \dot{P}$

PROBLEMS ALLEVIATED ??
NEW KEY INPUTS:

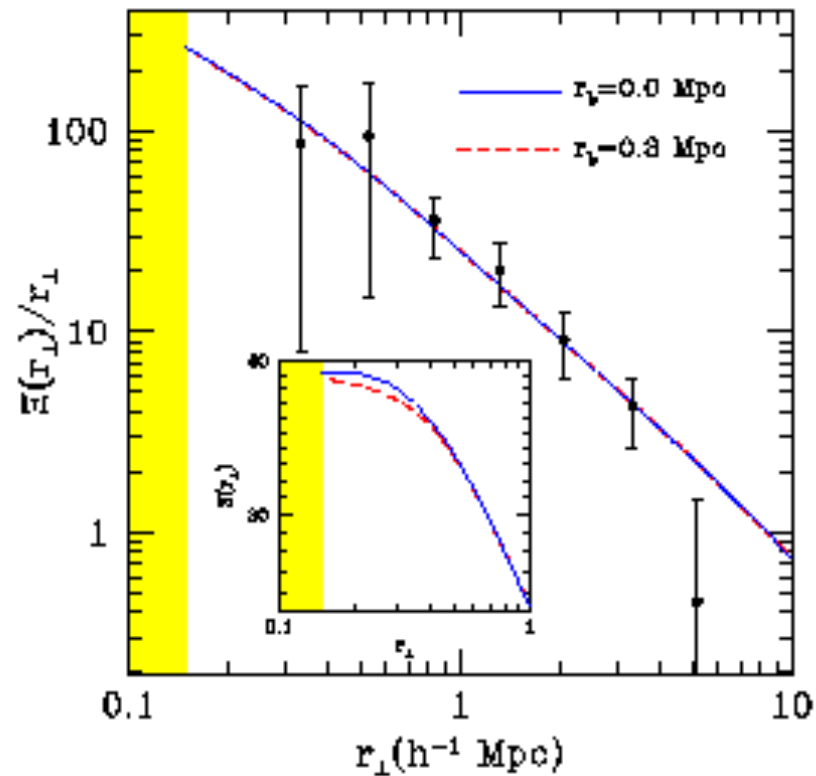
metal line cooling
Vel wind $\sim \sigma$ galaxy \times lum. factor



When did the IGM become enriched - I ?

EARLY METAL ENRICHMENT at $z > 6$

CIV-LBG cross correlation function



Porciani & Madau 2005

When did the IGM become enriched - II ?

Adelberger et al. 2005

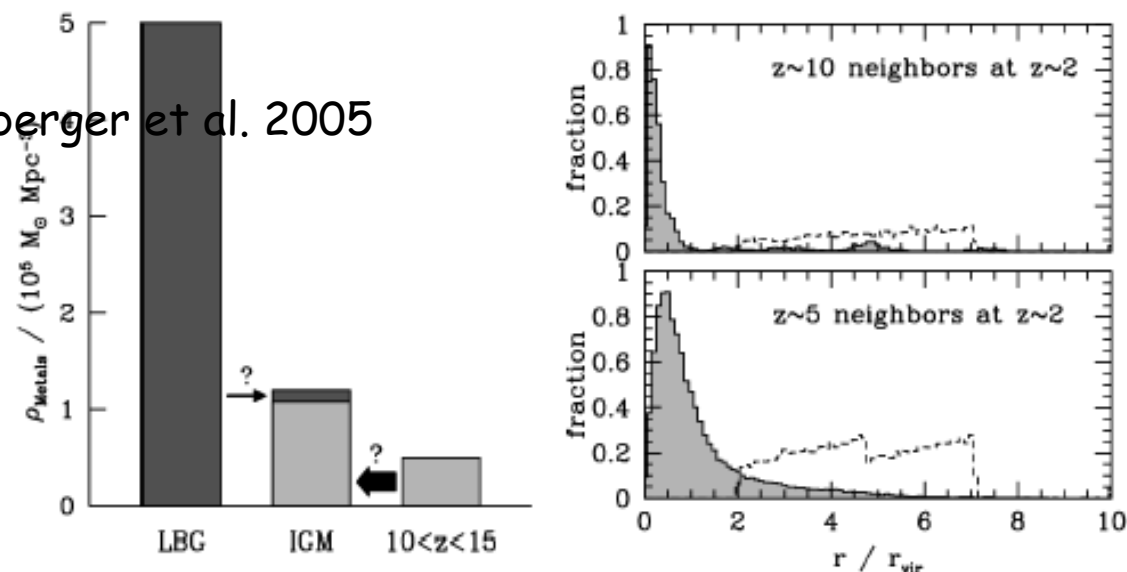
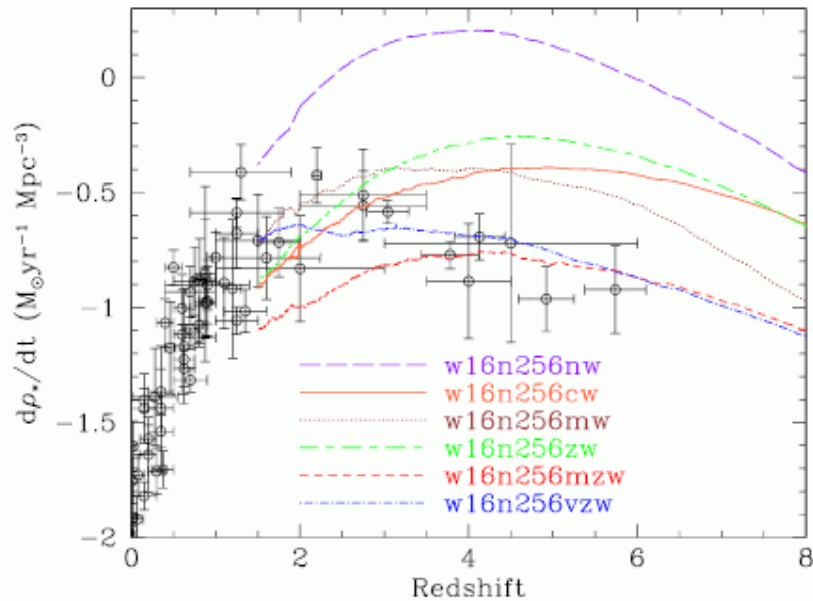


Figure 3. *Left panel:* The amount of metals produced in massive galaxies at $z \sim 2$ (LBG) compared to the amount of metals in the IGM at $z \sim 2$ and to the amount of metals produced at $10 < z < 15$. The amount of metals produced by massive galaxies at $z \sim 2$ was calculated by assuming that each $100M_{\odot}$ of star formation produced $1M_{\odot}$ of metals and scaling from the $z \sim 2$ stellar-mass density measured by Dickinson et al. (2003). An upper limit to the amount of metals produced at $10 < z < 15$ was derived by assuming a constant comoving star-formation density at all redshifts $2 < z < 15$. This implies that $\sim 10\%$ of the stars that exist at $z = 2$ were formed at $10 < z < 15$. It is an upper limit because the actual star-formation density at $z \gg 2$ appears to be significantly lower than the star-formation density at $z \sim 2$. The amount of metals in the IGM was calculated by multiplying the critical density by the estimated intergalactic metal density at $z \sim 2$, $\Omega_{\text{met}} \sim 4.4\Omega_C$ with $\Omega_C \sim 2 \times 10^{-7}$ (Schaye et al. 2003). If 90% of the intergalactic metals at $z \sim 2$ were produced at $10 < z < 15$, the fraction of metals that escape into the IGM would have to be ~ 100 times higher at $10 < z < 15$ than at $z \sim 2-3$. *Right panels:* Distance to the nearest massive ($M \gtrsim 10^{11}M_{\odot}$) halo at $z \sim 2$ for all GIF-LCDM simulation particles whose distance r to the nearest halo satisfied $2r_{\text{vir}} < r < 1h^{-1}\text{comovingMpc}$ at $z = 10$ (top) or $z = 5$ (bottom). Dashed lines show the particles' original (higher redshift) distribution of r/r_{vir} ; the solid shaded histograms show the distribution at $z \sim 2$. These particles initially lie at larger radii than those expected for the metals ejected by very high redshift winds, yet they mostly end up inside halos by $z \sim 2$. This implies that the metals ejected at $z \sim 5$ and $z \sim 10$ will generally also lie in massive halos at $z \sim 2$, not in the IGM.

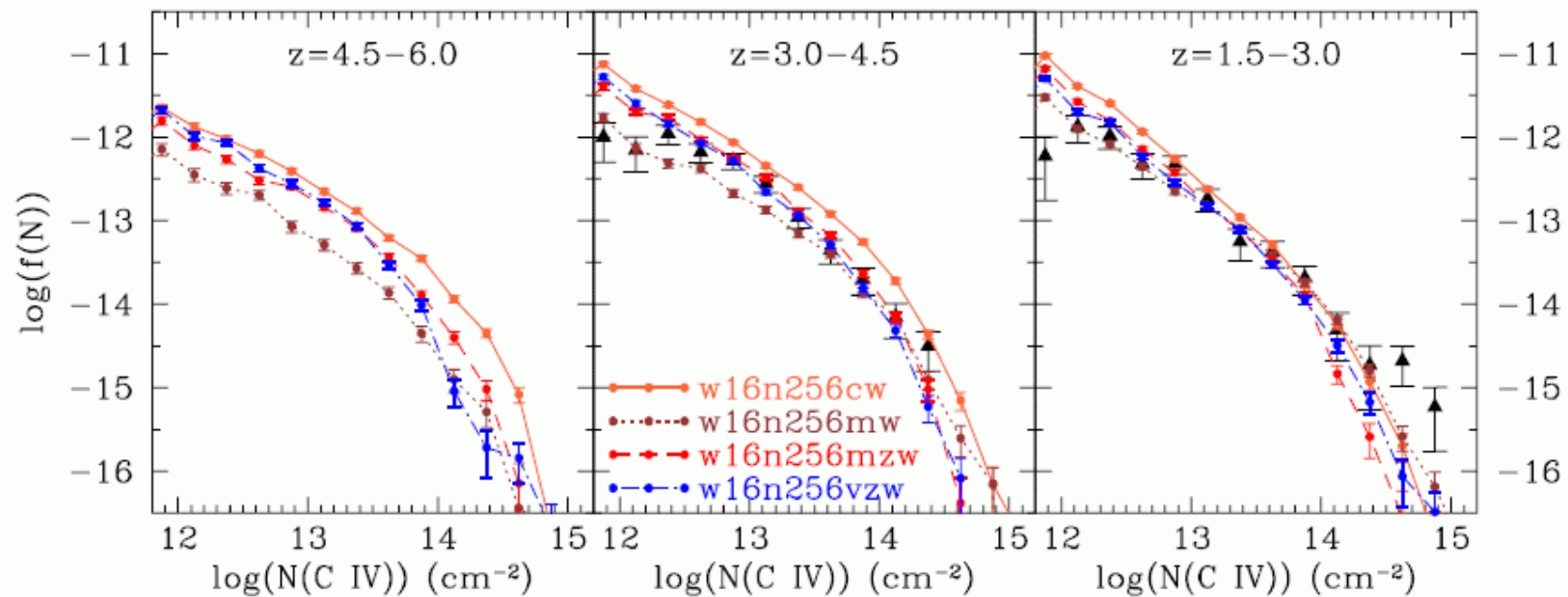
Perspectives - I

cw : constant speed wind
mw: momentum driven
nw: no wind



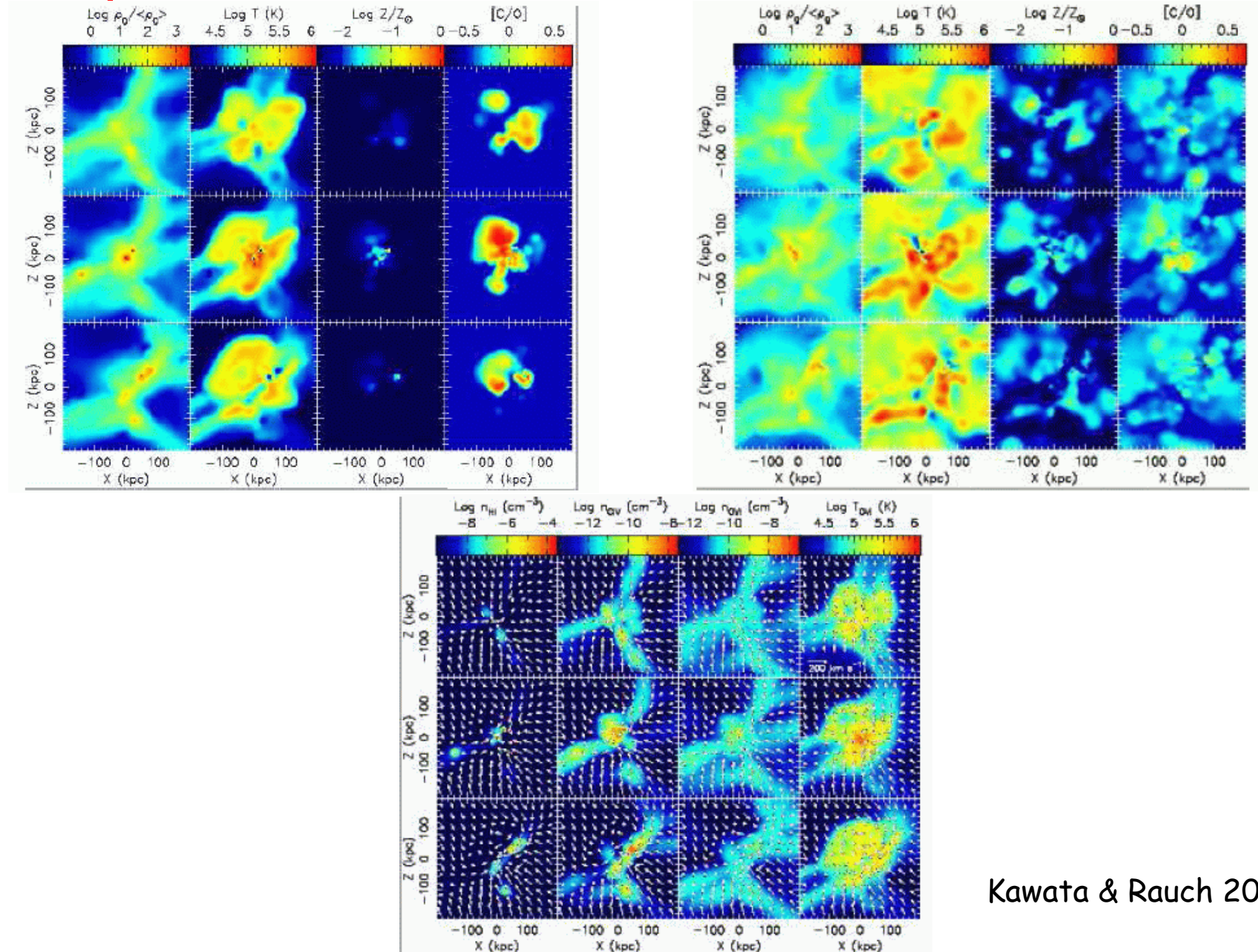
Exploring the parameter space...

(multi fitting as many observables
As possible SFR, HI evolution, CDDF...)



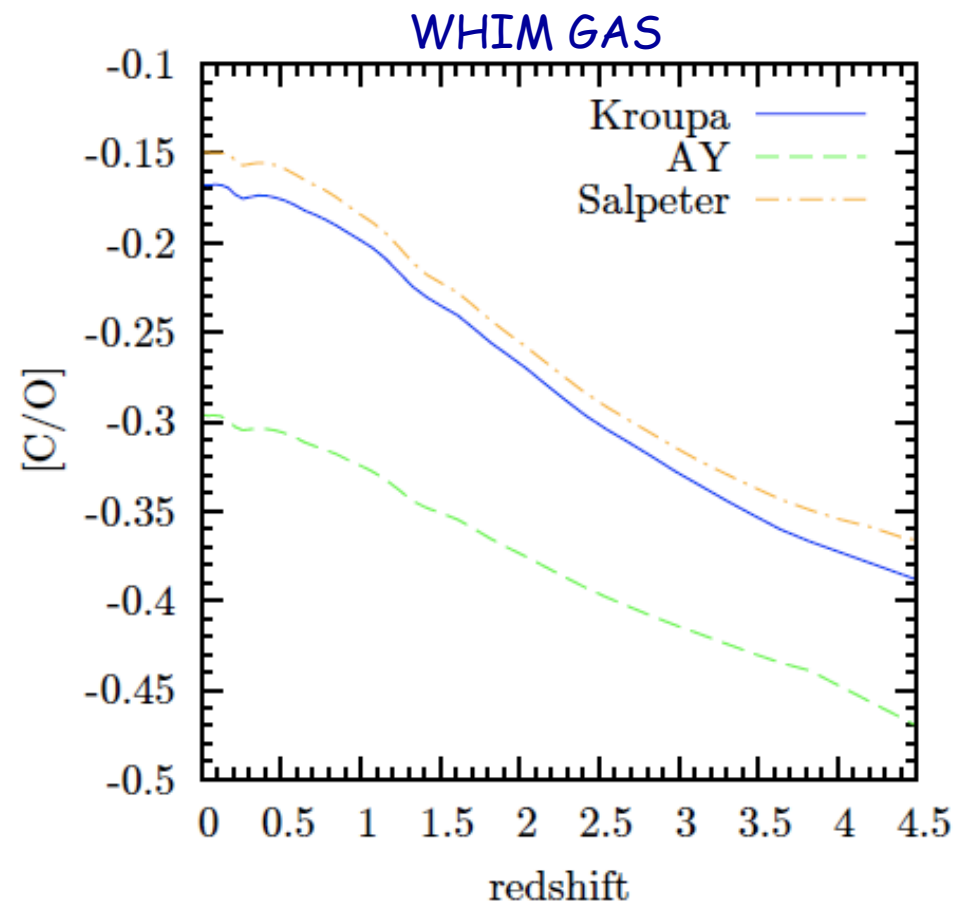
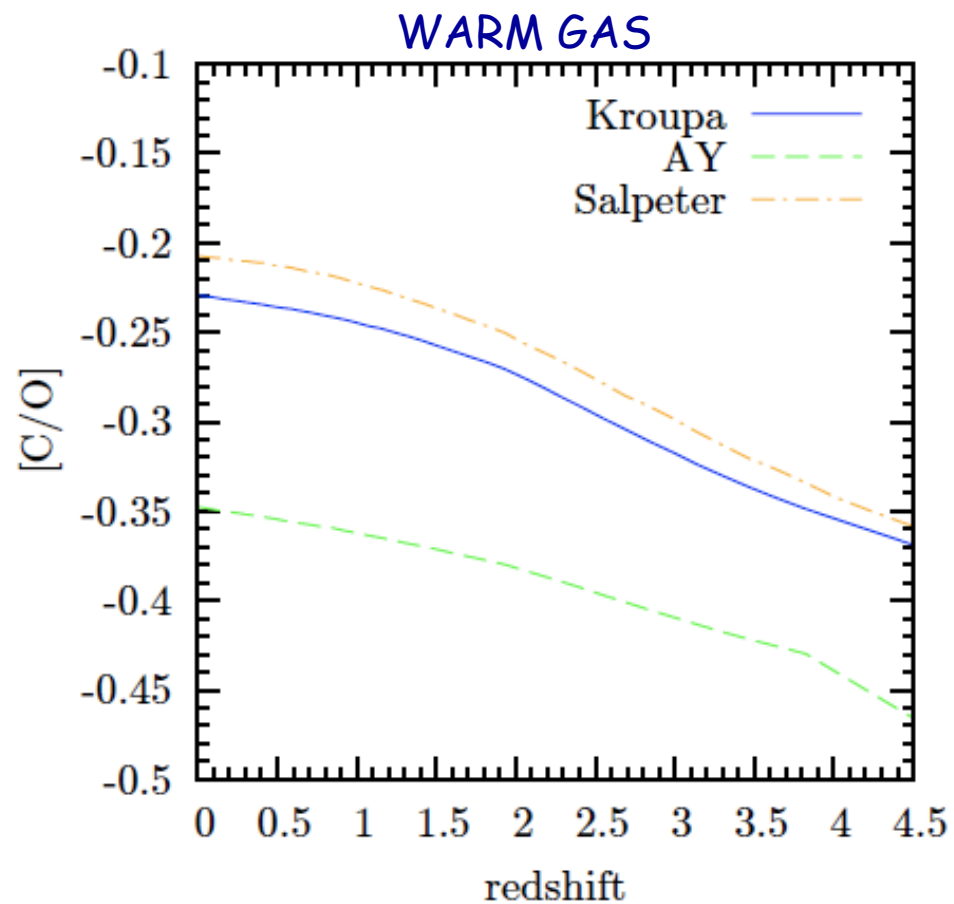
Perspectives -II

...with motivated chemodynamical models



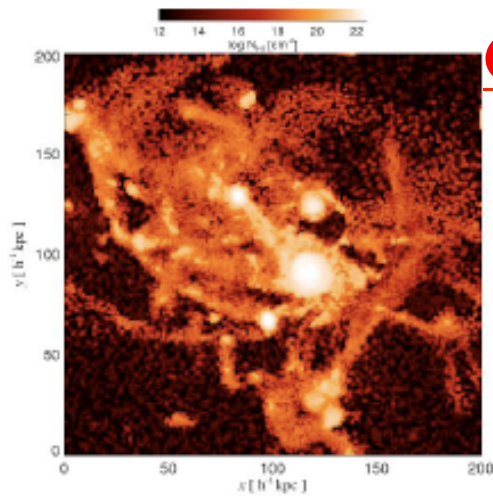
Kawata & Rauch 2007

Perspectives - III

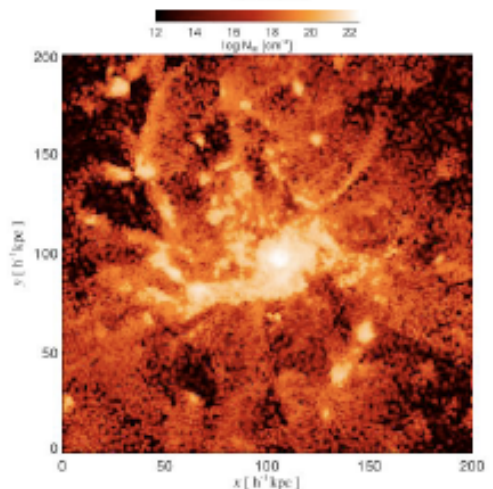


Tornatore, Borgani, Viel, Springel 2009

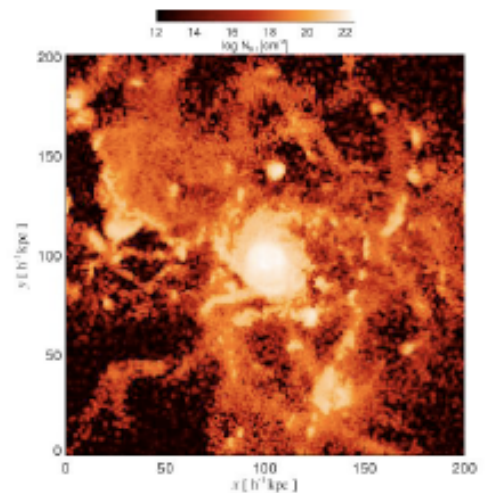
Galaxies/IGM: simulating galactic winds (HI)



Weak Winds

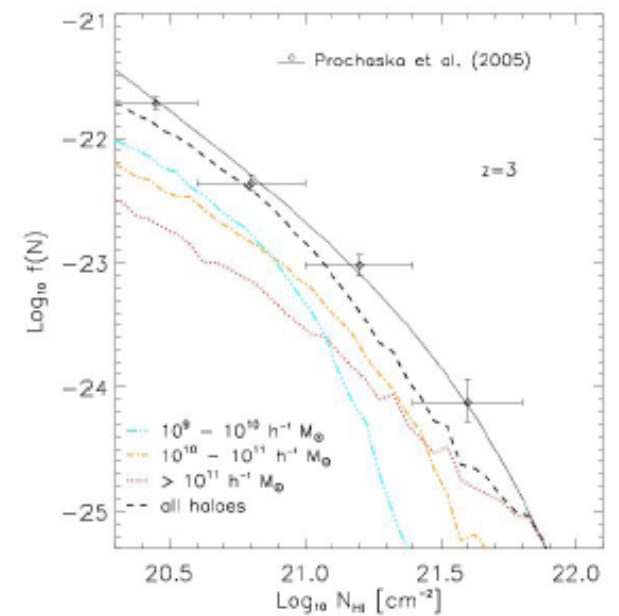
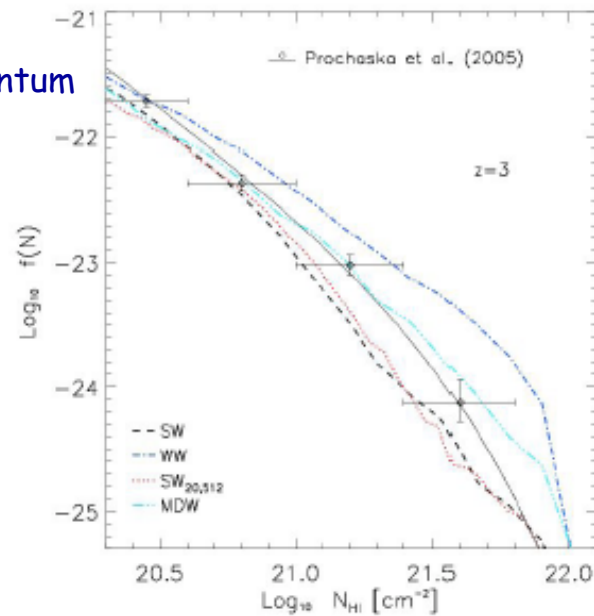


Strong Winds

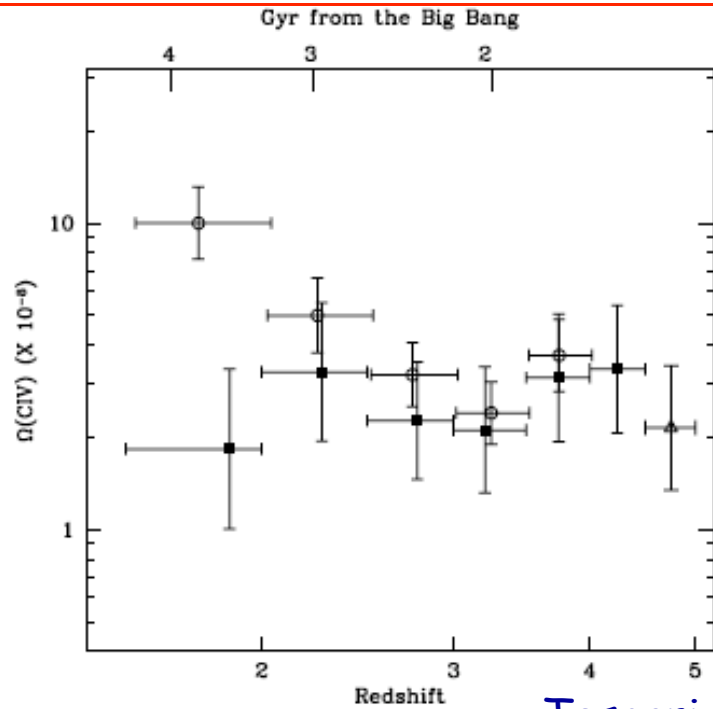


Momentum driven winds

Tescari, MV, Tornatore, Borgani, 2009

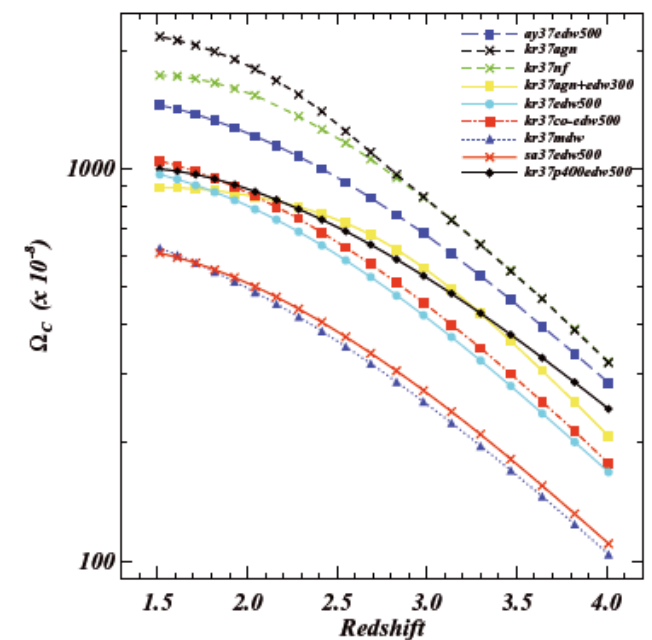
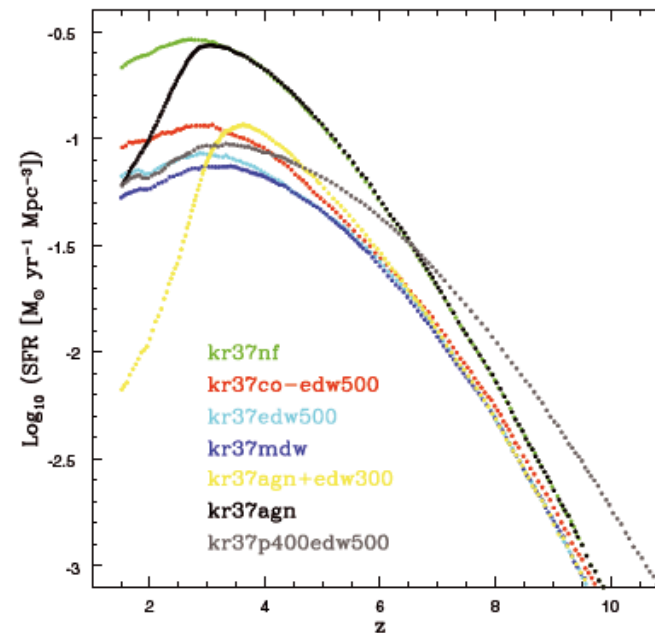


Galaxies and the IGM: cosmic evolution of the CIV

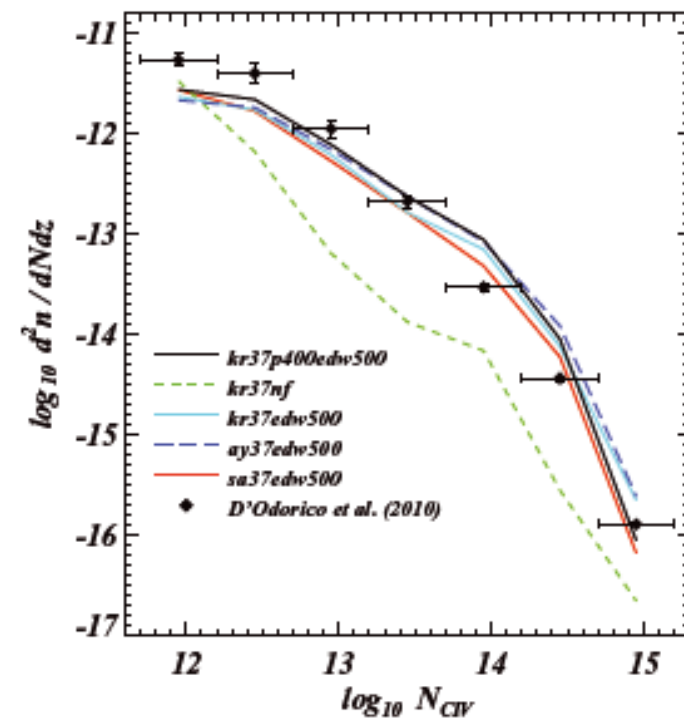
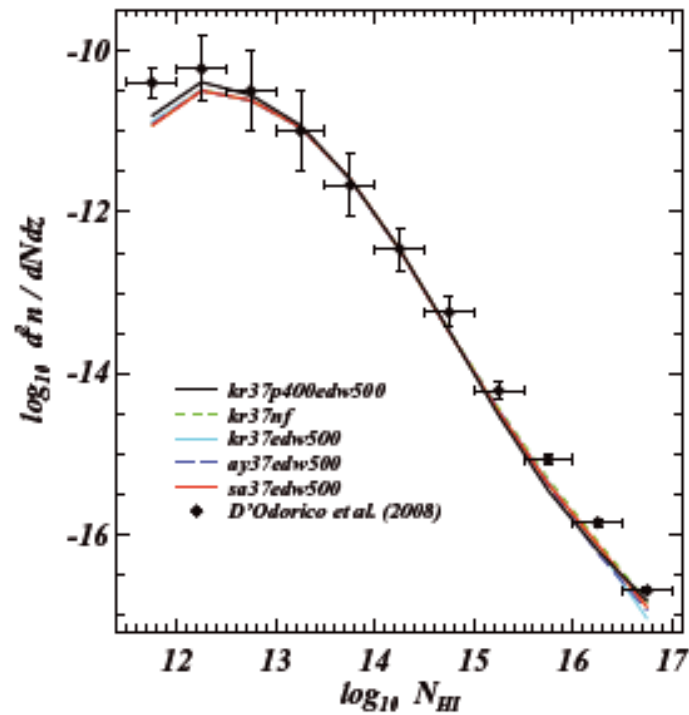


D'Odorico, Calura, Cristiani, MV 2010

Tescari, MV, D'Odorico, Cristiani, Calura, Borgani, Tornatore 2011

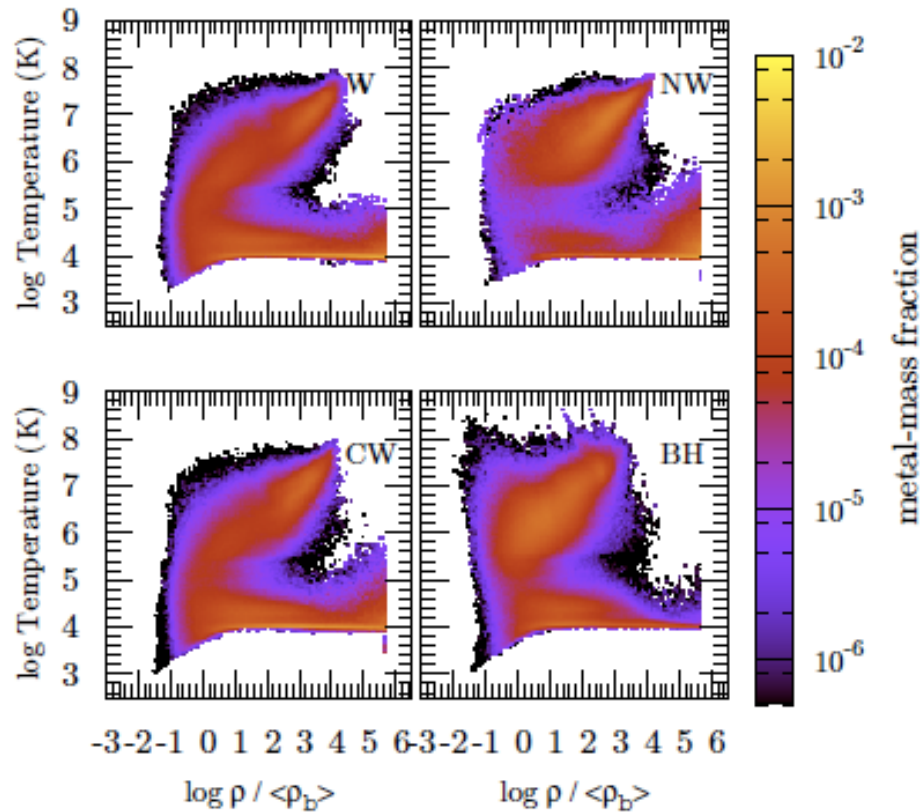


Galaxies and the IGM: HI and CIV CDDFs



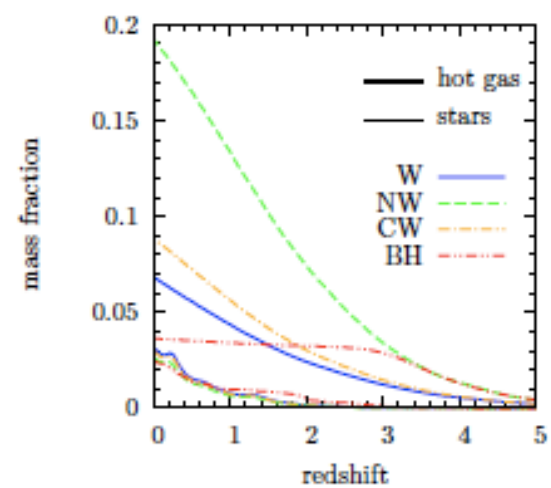
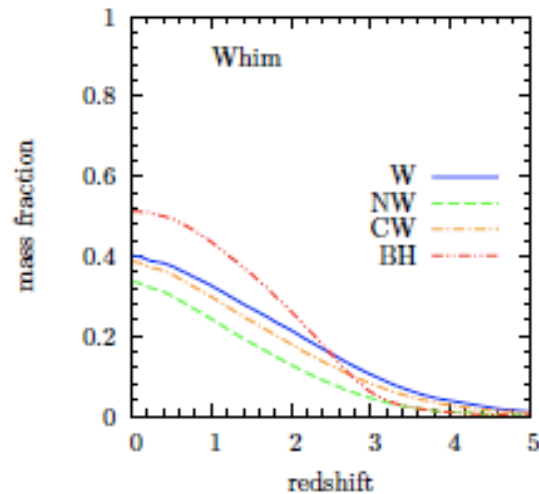
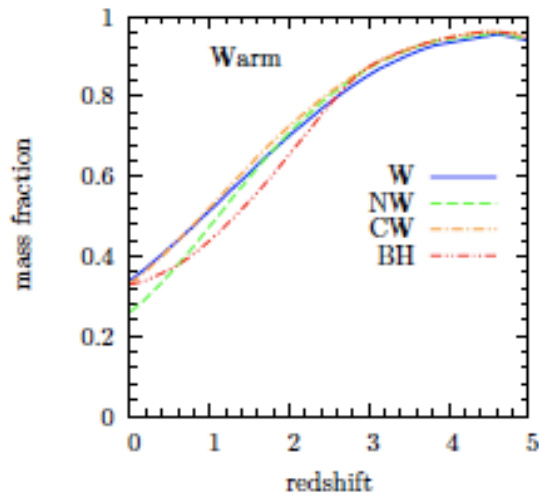
Effect of UVB also very important (see Nagamine, Choi, Yajima, 2010)

Galaxies and the IGM: low redshift evolution and feedback

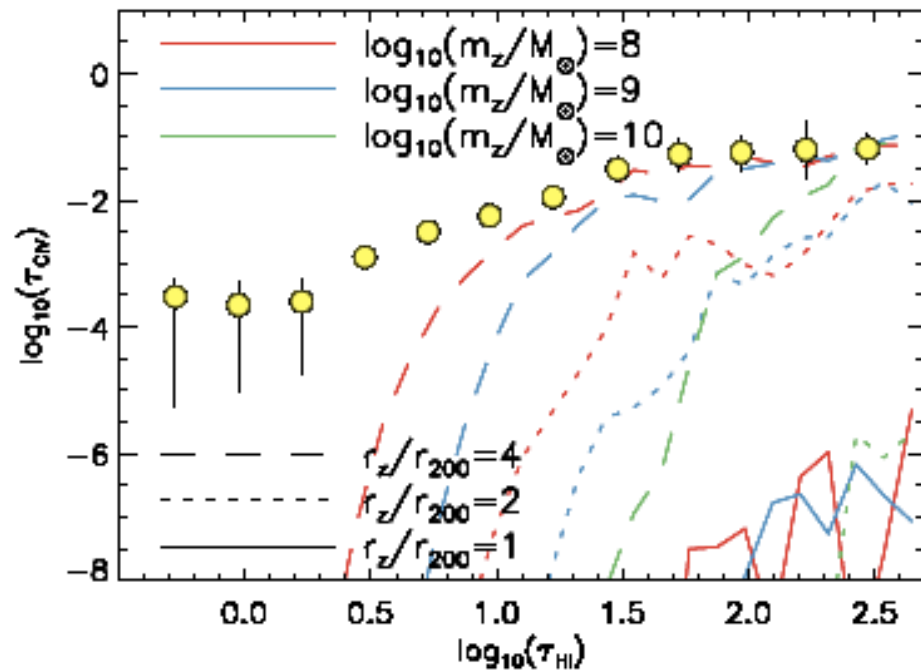


Tornatore, Borgani, Viel & Springel 2010

(see also Barai et al. 2010)



Galaxies and the IGM – VIII: IGM metallicity



Booth et al. 2010

Schaye and co-workers

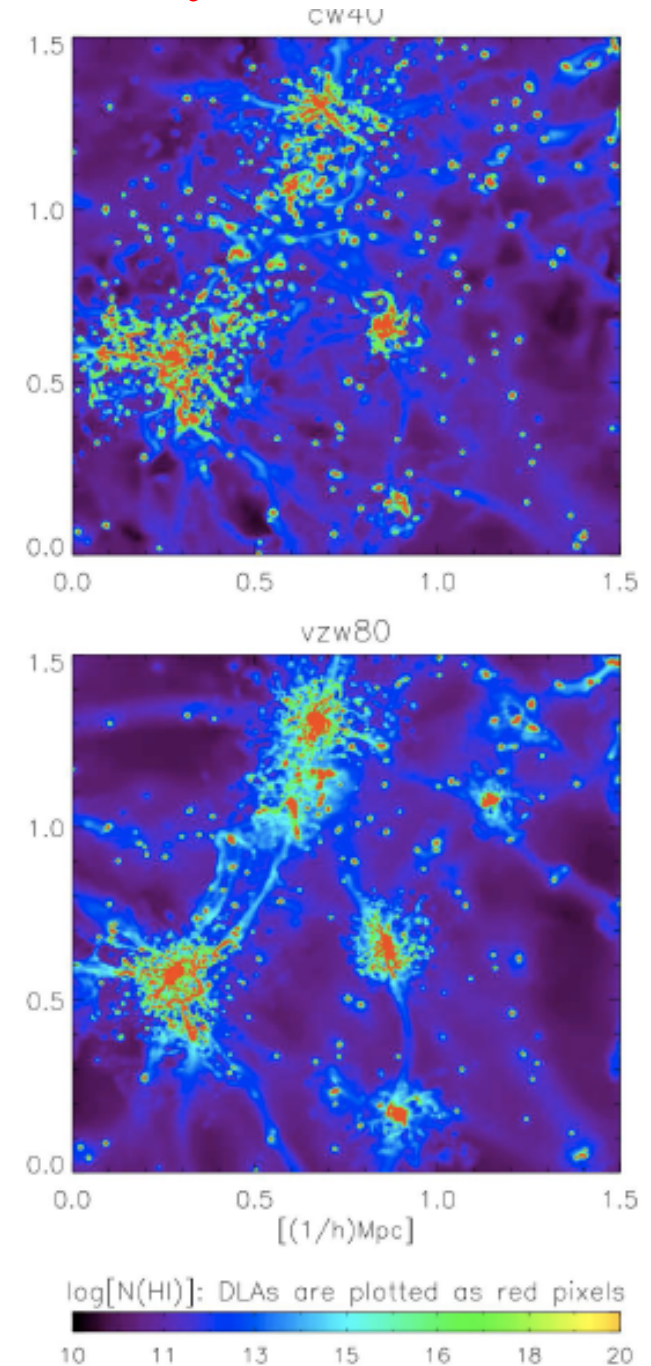
Nagamine and co-workers

Hong et al. 2010,

Cen et al. 2010,

Dave' and co-workers,

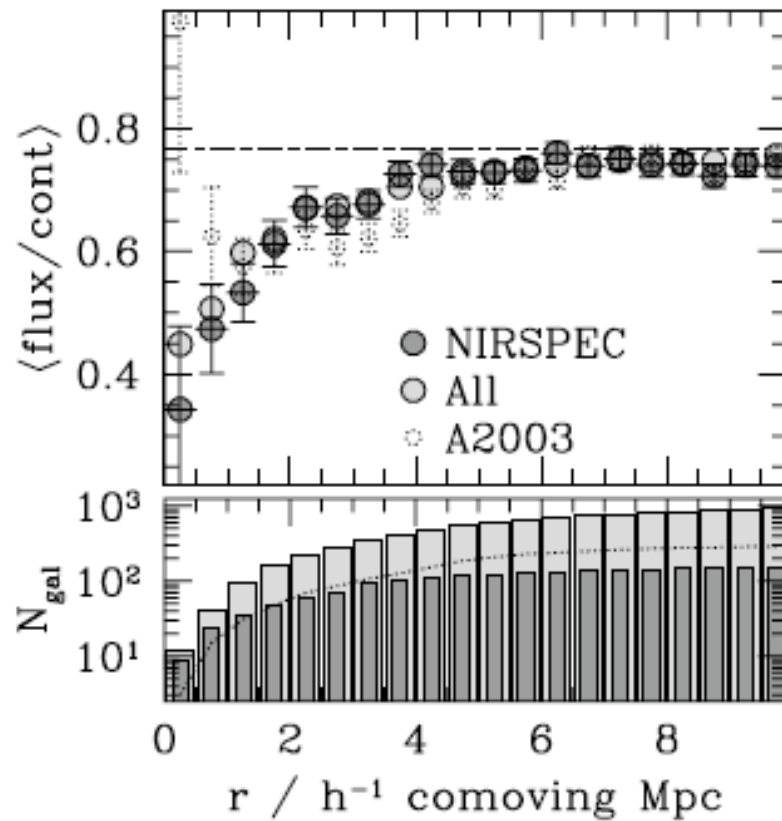
Tescari, MV et al 09, 10



Galaxies and the IGM – VI: observational results

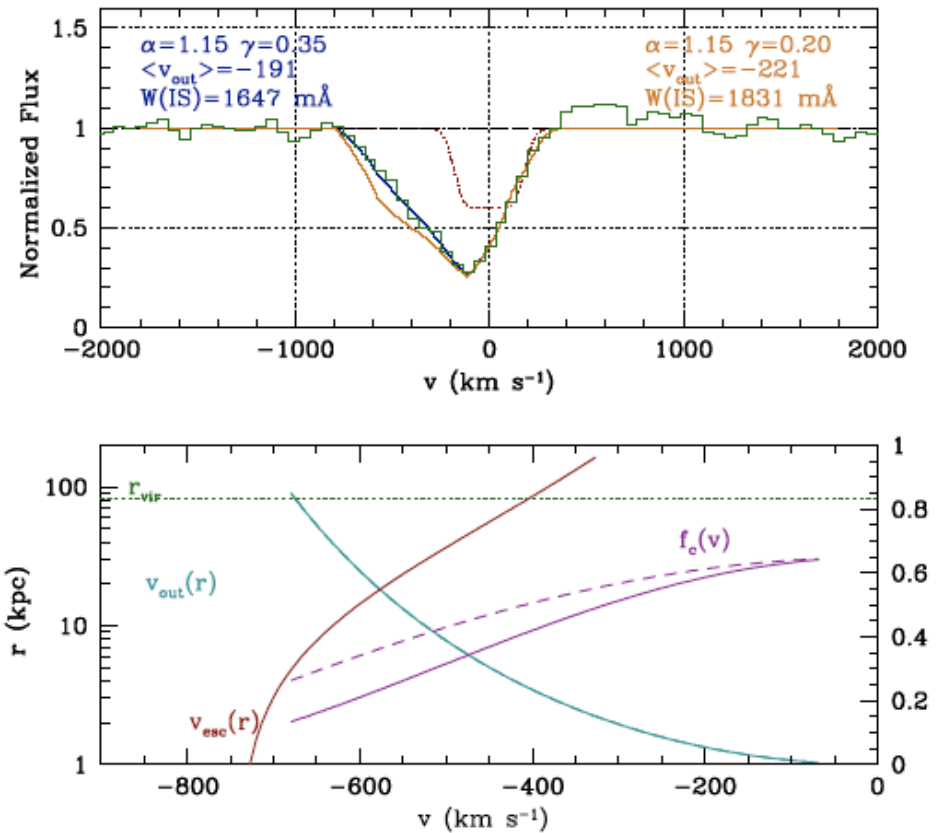
$$a(r) = Ar^{-\alpha}$$

$$f_c(r) \propto r^{-\gamma}$$



Adelberger et al. 2005

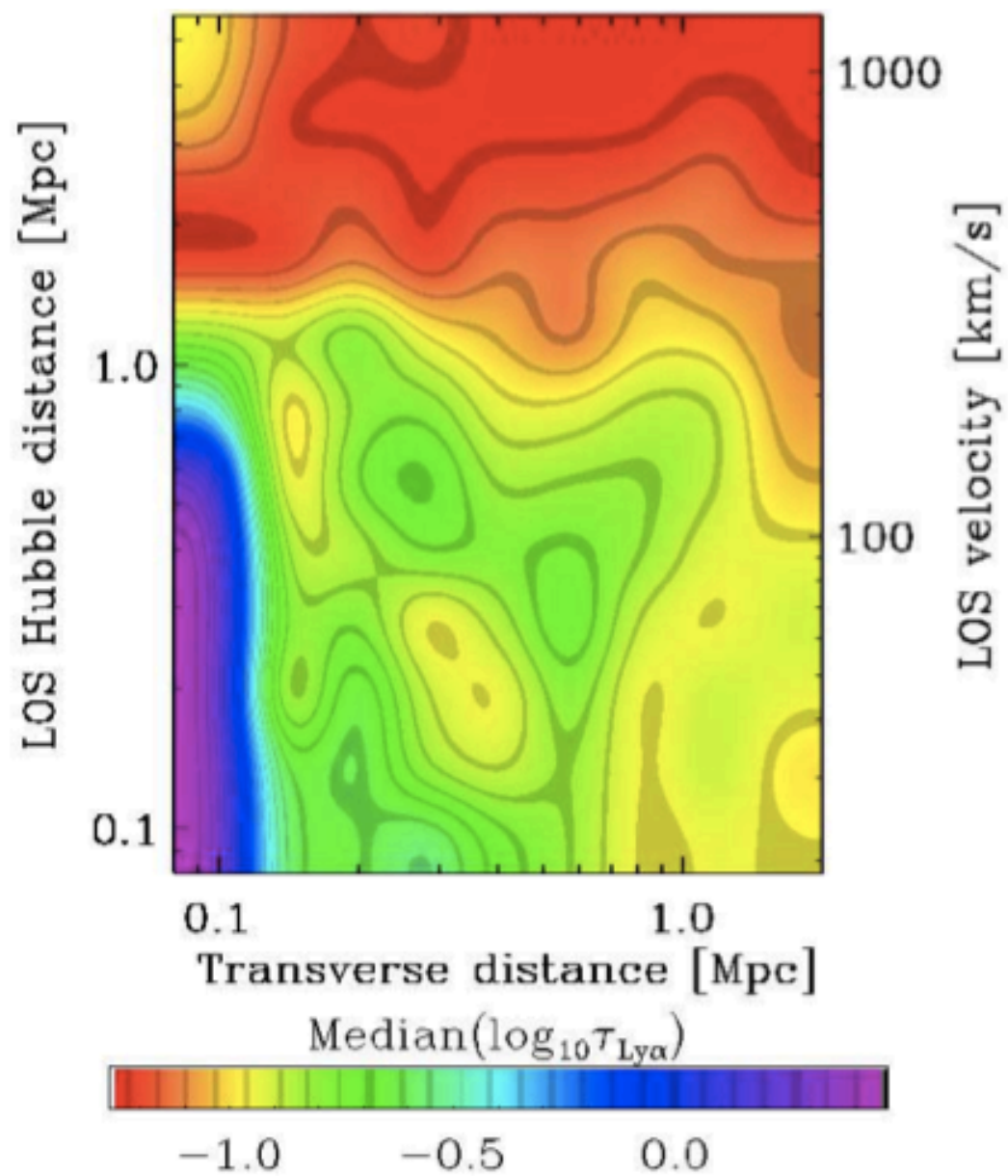
Background QSOs and foreground galaxies



Steidel et al. 2010

Background galaxies and foreground galaxies

Observational support for galactic outflows at high redshift



679
Galaxies

15
QSOs

SUMMARY ASTROPHYSICS

- Mechanism of metal enrichment of the IGM still unclear
metals in the simulations are too hot and too clumpy compared to observations
- Progress could be made by cross-correlation studies of IGM/galaxies
and observations of wind signatures in QSO pairs
- Nature and intensity of the UV background (not discussed here) somewhat clearer
- Insights from ISM community

